

Interface anisotropy in cobalt-based epitaxial superlattices

Hui He, C. H. Lee, F. J. Lamelas, W. Vavra, D. Barlett,^{a)} and Roy Clarke
Department of Physics, The University of Michigan, Ann Arbor, Michigan 48109

We have measured the magnetic anisotropy in a series of Co-Au and Co-Cu superlattices prepared by molecular-beam epitaxy. Significant epitaxial strains give rise to a magnetoelastic contribution and a large crossover thickness (~ 19 Å) for perpendicular easy magnetization. The results are discussed in the context of a careful analysis of the interfacial strains and coherence determined by *in situ* time-resolved reflection high-energy electron diffraction techniques and x-ray scattering.

The perpendicular anisotropy that appears in ultrathin magnetic films and multilayers presents an important and interesting topic not only for fundamental studies of magnetic properties^{1,2} in these low-dimensional structures³ but also for potential applications.⁴ The anisotropy can arise from several distinct mechanisms, including the broken symmetry of the structure at a surface, magnetocrystalline anisotropy, and magnetoelastic anisotropy. Surface or interface anisotropy¹ has been invoked as a mechanism for the perpendicular spin alignments in single layers,⁵ sandwich,⁶ and multilayer⁷⁻⁹ magnetic films.

In this paper we present the results of a series of measurements of magnetic anisotropy in epitaxial Co-Cu and Co-Au multilayer films grown¹⁰ by molecular-beam epitaxy (MBE) techniques. A comparison of these two systems is interesting in several respects. First, the lattice mismatch is much smaller in Co-Cu ($\sim 2\%$) than Co-Au ($\sim 14\%$). Second, Co is known to take up a metastable fcc structure¹¹ in the former superlattice whereas it is hcp in the latter. We have characterized the structural properties of these samples by x-ray scattering and *in situ* reflection high-energy electron diffraction (RHEED). Our results are analyzed with reference to the nature of the interface structure and its influence on the magnetic properties.

The Co-Au and Co-Cu superlattices were grown on (110) GaAs substrates in a Vacuum Generators V80 MBE system. Co layers were grown from an e-beam hearth at a rate of 0.3 Å/s. Individual Co layer thicknesses were controlled by integrating the signal from a quartz crystal thickness monitor. In this way, the effects of fluctuations in the Co deposition rate could be greatly reduced. Au and Cu were grown out of Knudsen cells with pyrolytic boron-nitride crucibles at rates of 0.080 ± 0.004 and 0.50 ± 0.025 Å/s respectively. In both series of superlattices, the Co layer thicknesses were chosen to span the range of 5 to 40 Å while Au and Cu thicknesses were fixed at 16 and 25 Å, respectively. The total superlattice film thickness was approximately 1500 Å in all cases.

RHEED patterns were recorded during the film growth using a specially developed charge-coupled device (CCD) detection system.¹² The image of the diffraction pattern from the film surface was digitized and stored in a microcomputer, facilitating analysis of line shapes and peak shifts in a time-resolved mode. The RHEED diffraction patterns from Co, Au, and Cu surfaces indicated that the superlattice

constituents were all well oriented within the growth plane. We find that fcc Au or Cu layers grow in the (111) orientation with Au or Cu $[1\bar{1}0]$ parallel to GaAs $[001]$. In the hcp Co-Au superlattices, Co $[11\bar{2}0]$ is parallel to GaAs $[001]$ in the plane of the substrate, while for the fcc Co-Cu samples Co $[1\bar{1}0]$ is parallel to Cu $[1\bar{1}0]$ and GaAs $[001]$. Well-ordered RHEED patterns were observed after just a few monolayers of Co growth on GaAs and the patterns remained distinct throughout the superlattice growth process.

The technique mentioned above permits measurement of the spacing and widths of RHEED streaks as a function of growth time on a submonolayer level. Intensity scans across the specular beam and diffraction streaks were recorded with the electron beam along Co $[11\bar{2}0]$ and Au $[1\bar{1}0]$ axes during growth. Shown in Fig. 1(a) are examples of measured intensities across RHEED streaks at different stages of the growth of a Co-Au bilayer. RHEED streak positions obtained from such scans [Fig. 1(b)] show that the development of the spacing of the RHEED streaks is very different during the growth of Co and Au layers. The Au streak spacing relaxes to a constant value after just one monolayer (ML) of Au is deposited on Co [Fig. 1(b)], indicating that the Co-Au interface is atomically abrupt. On the other hand, during the deposition of Co on Au, the lattice spacing of Co relative to the Au spacing is seen to decrease gradually. The linewidth of the Co streaks is generally broader than that of Au streaks; in fact the Co in-plane coherence seems to deteriorate progressively beyond ~ 3 ML Co. These results demonstrate the usefulness of digital time-resolved RHEED techniques for quantitative measurements of the growth dynamics, particularly at the interface. From the plot of the RHEED streak spacing as a function of growth time [Fig. 1(b)], we estimate the lattice mismatch between the last Co ML and the subsequent Au layer deposited on top of it is approximately 5.5%. However, the RHEED technique is a probe of the uppermost surface; upon subsequent deposition of additional layers, the structure is expected to relax so that the strain measured by RHEED in the free surface may not accurately reflect the final distribution of strains in the sample after growth.

In order to obtain values of strain which are representative of the final relaxed structure, we carried out x-ray scattering measurements on the as-grown samples. Our measurements, performed on a four-circle diffractometer, confirm the epitaxial relationship given above and also provide information on the interfacial quality and epitaxial strains. Figure 2(a) shows an out-of-plane x-ray scan on a

^{a)} Applied Physics Program.

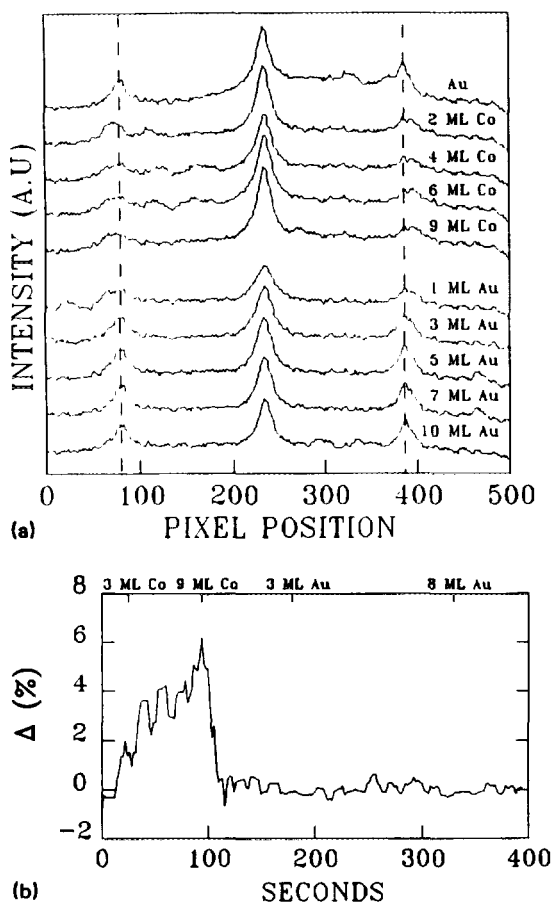


FIG. 1. (a) Representative RHEED streak intensities recorded using a CCD detector at different stages of Co-Au bilayer growth. The central peak is the specular beam. Such scans were recorded every 2 s, corresponding to ~ 0.07 ML of Au and ~ 0.2 ML of Co. Not all data recorded are shown. (b) The relative spacing, Δ (inversely proportional to the lattice parameter), of the RHEED streaks as a function of growth time.

Co-Au superlattice fit with a model which includes interface roughness.¹⁰ From the fit, we deduce an average interface width of 2 ML. Similar results were obtained for the Co-Cu superlattices. We have also performed x-ray scans in transmission geometry with the scattering vector parallel to the plane of the sample; these scans are used to determine epitaxial relationships and strains. The in-plane epitaxial strains were determined from peak positions in scans through the Au [220] and the Co [1120] peaks [Fig. 2(b)]. We find that as the Co layer thickness is increased the tensile strain in the Co layers is relaxed, while the compressive strain present in the Au layers remains relatively constant. The difference between the values of strain measured by RHEED and x-ray techniques suggests that some relaxation takes place during or after growth of the superlattice.

Magnetic measurements¹³ were performed using a Quantum Design MPMS SQUID magnetometer. Figure 3 shows the behavior of hysteresis loops at 300 K for various thicknesses of Co layers with applied fields perpendicular and parallel to the film plane. It is clear from Fig. 3 that the easy axis of magnetization shifts out of the film plane when the Co layer thickness decreases. The effective anisotropy

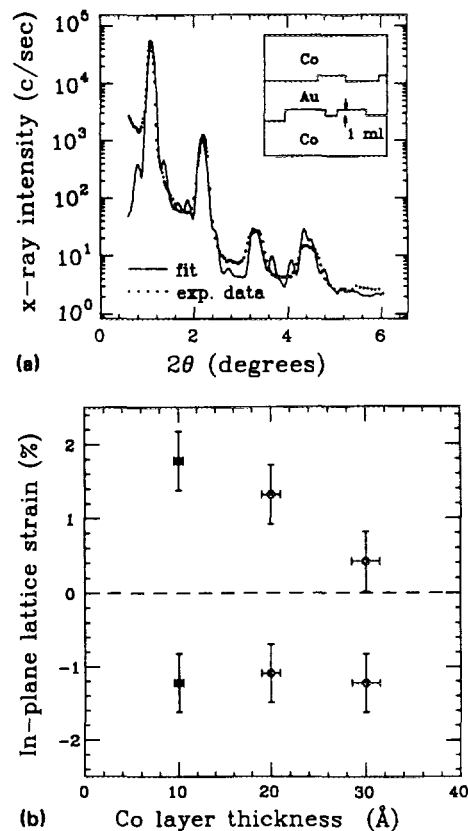


FIG. 2. (a) Low-angle 00/x-ray scan data of Co(20 Å)-Au(16 Å) superlattice and calculated intensity (solid line) from a model shown schematically in the inset. (b) In-plane epitaxial strains of Co and Au layers, plotted as a function of Co layer thickness. Co strains are tensile (upper points) and Au strains are compressive (lower points). Values of the strain are given relative to bulk lattice spacings.

K_{eff} is defined as $(1/V) \int_0^{H_{\text{sat}}} (M_{\perp} - M_{\parallel}) dH$, where V is the film volume. Plotting $K_{\text{eff}} \Lambda$ versus the Co layer thickness (Fig. 4), where Λ is the superlattice periodicity, we get crossover thicknesses for Co-Au and Co-Cu of 19 and 11 Å, respectively, below which the easy axis is perpendicular to the layers.

A recent model by Chappert and Bruno¹⁴ is used here to discuss the magnetic anisotropies of Co-based superlattices in connection with RHEED and x-ray scattering results. The magnetoelastic contribution to the anisotropy is $K^{\text{ME}} = B\epsilon$, where B is a magnetoelastic constant (for bulk Co, $B = 5 \times 10^6$ erg/cm³), and ϵ is the strain.¹⁴ From the x-ray scattering measurements we obtain $\epsilon \sim 1.75\%$ in a Co-Au superlattice with 10-Å-thick Co layers, resulting in a value of $K^{\text{ME}} = 8.75 \times 10^6$ erg/cm³. This value of K^{ME} , in combination with the magnetocrystalline anisotropy (5.56×10^6 erg/cm³) and shape anisotropy (-13.0×10^6 erg/cm³) of hcp Co, yields a total anisotropy of 1.31×10^6 erg/cm³. This is comparable to the value from our magnetization measurement. In the Co-Cu films, the measured anisotropies are smaller than in Co-Au, although the strains measured by x-ray methods are nearly equal.¹¹ This difference may be accounted for¹³ by adjustments of the magnetocrystalline and magnetoelastic constants. In conclusion, we have shown the usefulness of careful measurements of lattice

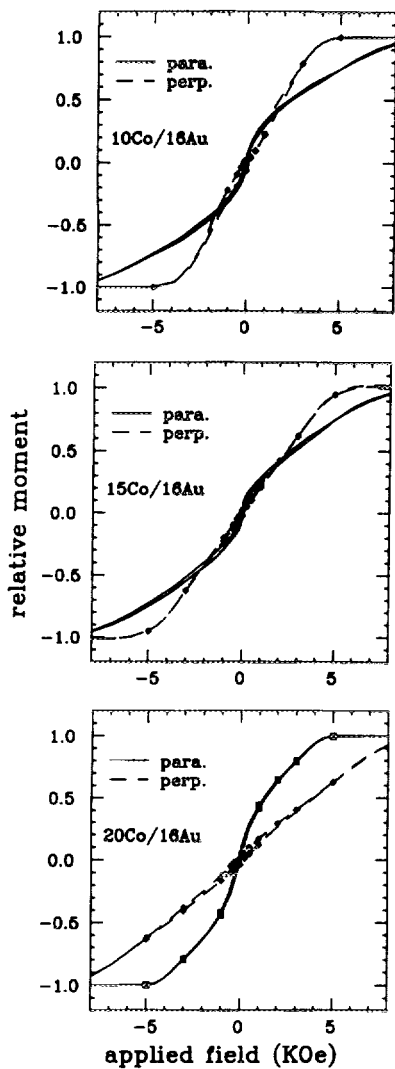


FIG. 3. Magnetization hysteresis loops for a constant Au thickness (16 \AA) series of Co-Au superlattices measured at $T = 300 \text{ K}$. Fields were applied perpendicular and parallel to the film plane.

strains using a combination of x-ray scattering and RHEED techniques. In the case of Co-Au and Co-Cu, the epitaxially induced strains that arise at the interfaces are sufficient to account for the observed perpendicular anisotropies.

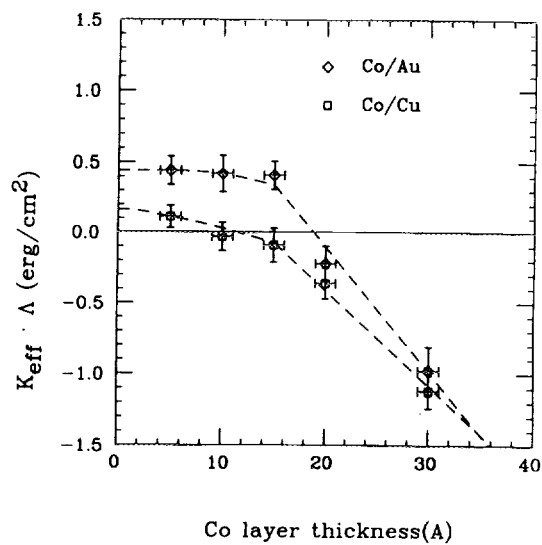


FIG. 4. Anisotropy energy of Co-Au and Co-Cu superlattices as a function of Co layer thickness at $T = 300 \text{ K}$.

This work was supported in part by National Science Foundation Grant No. DMR-8805156.

¹For a review, see for example, U. Gradmann, in *Thin Film Growth Techniques for Low-Dimensional Structures*, edited by R. F. C. Farrow, S. S. P. Parkin, P. J. Dobson, J. H. Neave, and A. S. Arrott (Plenum, New York, 1987).

²J. G. Gay and R. Richter, *Phys. Rev. Lett.* **56**, 2728 (1986).

³C. L. Fu, A. J. Freeman, and T. Oguchi, *Phys. Rev. Lett.* **54**, 2700 (1985).

⁴See, for example, S. Iwasaki and Y. Nakamura, *IEEE Trans. Magn. Mater.* **MAG-13**, 1272 (1977); W. B. Zeper, F. J. A. M. Greidanus, P. F. Garcia, and C. R. Fincher, *J. Appl. Phys.* **65**, 4971 (1989).

⁵C. Liu, E. R. Moog, and S. D. Bader, *Phys. Rev. Lett.* **60**, 2422 (1988).

⁶C. Chappert, K. Le Dang, P. Beauvillain, H. Hurdequint, and D. Renard, *Phys. Rev. B* **34**, 3192 (1986).

⁷P. F. Garcia, A. D. Meinhaldt, and A. Suna, *Appl. Phys. Lett.* **47**, 178 (1985).

⁸H. J. G. Draaisma and W. J. M. Dejonge, *J. Magn. Magn. Mater.* **66**, 351 (1987).

⁹F. J. A. den Broeder, D. Kuiper, A. P. van de Mosselaer, and W. Hoving, *Phys. Rev. Lett.* **60**, 2769 (1988).

¹⁰C. H. Lee, H. He, F. J. Lamelas, W. Vavra, C. Uher, and R. Clarke, *Phys. Rev. Lett.* **62**, 653 (1989).

¹¹F. J. Lamelas, C. H. Lee, H. He, W. Vavra, and R. Clarke, *Phys. Rev. B* **40**, 5837 (1989).

¹²D. Barlett, H. He, C. H. Lee, F. J. Lamelas, and R. Clarke (unpublished).

¹³C. H. Lee, F. J. Lamelas, H. He, W. Vavra, C. Uher, and R. Clarke (unpublished).

¹⁴C. Chappert and P. Bruno, *J. Appl. Phys.* **64**, 5736 (1988).